

Hydration of DOPC bilayers by differential scanning calorimetry

Anne S. Ulrich¹, Malkit Sami, Anthony Watts^{*}

Department of Biochemistry, University of Oxford, South Parks Road, Oxford OX1 3QU, UK

(Received 22 June 1993)

Abstract

The phase diagram of the unsaturated lipid dioleoylphosphatidylcholine (DOPC) in aqueous multibilayer dispersions has been constructed from a series of differential scanning calorimetry (DSC) thermograms over the temperature range from -40 to $+10^{\circ}\text{C}$, covering a range of hydration levels from the monohydrate to excess free water. Both the lipid chain melting transition and the ice melting point are found to be hydration dependent. From their respective variations it is found that the bilayer in the gel phase binds approximately 9 H_2O per lipid, while the liquid-crystalline state has a saturation limit near 20 H_2O . The water transition exhibits a hydration-dependent melting point depression, which can be explained in terms of newly incorporated water between the bilayer surfaces upon melting of the acyl chains, and which is reminiscent of the events that occur at the pre-transition for saturated lipids. From the melting point depression, the thermodynamic activity of the interbilayer water can be calculated and thus the repulsive hydration force characterized quantitatively. We evaluate a (non-isothermal) hydration force decay constant around 2.8 H_2O , which demonstrates that this DSC approach is well-suited for quantitatively characterizing the hydration properties of unsaturated lipid dispersions at low temperature.

Key words: Lipid hydration; Differential scanning calorimetry; Phase diagram; Dioleoylphosphatidylcholine bilayer; Unsaturated chain; Freezing point depression; Hydration force

1. Introduction

Biological membranes undergo various morphological changes and can suffer considerable damage as a consequence of freezing, dehydration or a combination of both effects [1,2]. For a better understanding of the anhydro- and cryo-characteristics of lipid bilayers, it is necessary to investigate the phase behaviour and the hydration characteristics of the principal membrane constituents. Phase diagrams have been constructed for various saturated phospholipids over wide ranges of

temperature and composition [3–12]. However, less information is available for unsaturated model membranes [2,13,14]. In the present study we have carried out a systematic thermal analysis of the hydration properties of dioleoylphosphatidylcholine (DOPC) multibilayers, using differential scanning calorimetry (DSC) to monitor both the lipid chain-melting transition as well as the ice-to-water transition as a function of water content. Insight into the nature of these transitions will be provided by direct observation of their hydration dependence, and the resulting phase diagram will be compared and contrasted with that of saturated phosphatidylcholine analogues.

The thermal behaviour of an unsaturated lipid with a phase transition temperature below zero degrees is expected to differ from that of saturated lipids. That is because the melting of the unsaturated acyl chains in DOPC occurs in the presence of frozen ice rather than liquid water. We find that the lipid unsaturation, in turn, has a pronounced effect on the transition temperature of the ice and causes it to melt significant below zero degrees. From the melting point depression of the water, thermodynamic information can be deduced

^{*} Corresponding author. Fax: +44 865 275259.

¹ Present address: European Molecular Biology Laboratory, POB 102209, 69012 Heidelberg, Germany.

Abbreviations: DSC, differential scanning calorimetry; DOPC, dioleoylphosphatidylcholine; DPPC, dipalmitoylphosphatidylcholine; ^2H -NMR, deuterium nuclear magnetic resonance spectroscopy; n_{w} , number of water molecules per lipid; a_{w} , water activity; P , hydration pressure; P_0 , nominal pressure at zero hydration; ν , hydration force decay constant; $T(n_{\text{w}})$, ice melting transition with freezing point depression; T_0 , melting point of pure water; ΔH_{m} , melting enthalpy of ice; V_{w} , molar volume of water.

about the exponentially decaying hydration force which is known to dominate the repulsion between bilayers over distances of up to 30 Å [1,6,15–21]. The potential of using the ice melting transition, monitored by ^2H -NMR or X-ray diffraction, as a measure of hydration forces in bilayers has recently been appreciated [22,23] and the present DSC study thus constitutes another method for the characterization of hydration forces [24].

2. Materials and methods

Commercial DOPC (Sigma) in chloroform was dried first under a stream of nitrogen and then under high vacuum at room temperature (48 h), so that the monohydrate is obtained [7]. For each sample approx. 10 mg of the dried DOPC was placed in a pre-weighed large-volume aluminium sample pan, and a well-defined amount of doubly distilled water was added (Hamilton microsyringe) to obtain the desired hydration level. The DSC pans were immediately sealed and left to equilibrate for approx. 48 h at room temperature, above their chain melting transition. Multilamellar liposomes with different hydration levels were thus formed spontaneously, with well-defined water/lipid ratios in the range of $1 \leq n_w \leq 30 \text{ H}_2\text{O}$ per lipid ($\pm 0.3 \text{ H}_2\text{O}$).

Thermograms of the DOPC samples were recorded on a Perkin-Elmer DSC 7 differential scanning calorimeter, using an empty pan as a reference. The samples were scanned from -40°C to $+10^\circ\text{C}$ at a heating rate of 2° per min, and no significant differences were observed for variations in the heating rates between 1° and 4° per min. A heating scan was recorded after equilibrating the sample at -40° for about 10 min, followed by a cooling run and a repeated heating. No differences were observed between the first and second heating scans and the samples could be stored at 4°C for several weeks with reproducible results. Typically, the DSC thermograms showed the smooth appearance of a well-defined phase transition, thus confirming that the DOPC samples were well equilibrated and homogenous. Any sample which did not give a smooth transition was discarded and the experiment repeated with a fresh preparation. Samples were analyzed by TLC to check for any lysolipid, and no degradation was observed as the lipid gave a single spot in $\text{CHCl}_3/\text{MeOH}/25\%\text{NH}_4\text{OH}$ (65 : 30 : 3, v/v/v) on silic acid plates.

3. Results and discussion

A series of heating thermograms were obtained by DSC for DOPC with different water/lipid ratios n_w

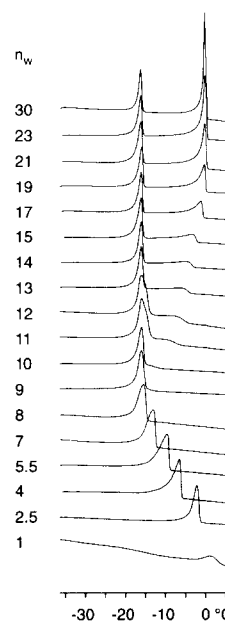


Fig. 1. Representative heating thermograms of DOPC multibilayers ($\sim 10 \text{ mg}$ of lipid) with different water/lipid ratios (n_w) between 1 and 30 H_2O per lipid, in the temperature range from -40 to $+10^\circ\text{C}$. The thermograms are not plotted to scale but are normalized to the height of the lipid phase transition.

from 1 to 30 H_2O molecules per lipid, as shown in Fig. 1. At low hydration levels ($n_w \leq 9 \text{ H}_2\text{O}$) a single endothermic transition is observed in all samples, which is the gel to liquid-crystalline phase transition arising from the acyl chain-melting of the lipid. Above $n_w \geq 10 \text{ H}_2\text{O}$, two types of transitions can be discerned, namely the lower lipid phase transition and an ice melting peak at higher temperature which is initially manifest as a shoulder to the lipid transition. For hydration levels up to $n_w \leq 9 \text{ H}_2\text{O}$, the lipid chain-melting transition is seen to occur at successively lower temperatures from about 4°C for the monohydrate down to -16.5°C , which corresponds to the literature value for fully hydrated DOPC [2,14], with a molar transition enthalpy of 8.7 kcal/mol . A similar hydration dependence of the gel to liquid-crystalline phase transition temperature has been characterized for a variety of saturated and unsaturated phospholipids [2–12]. Once the acyl chain-melting transition has reached its limiting temperature with hydration (16.5°C , $n_w \approx 9 \text{ H}_2\text{O}$), a shoulder emerges on the right-hand side of the main transition as seen in Fig. 1 for $n_w \geq 10 \text{ H}_2\text{O}$. Over the range of $10 \leq n_w \leq 20 \text{ H}_2\text{O}$, this shoulder gradually extends towards higher temperatures and grows into a distinct peak that moves to a limiting value at 0°C . This transition must be due to the melting of ice, which exhibits a remarkable melting point depression of up to 13 degrees in the presence of DOPC. The low-temperature edge of the ice transition is significantly broadened, indicating that there exists a range of contributions from portions of water with continually depressed

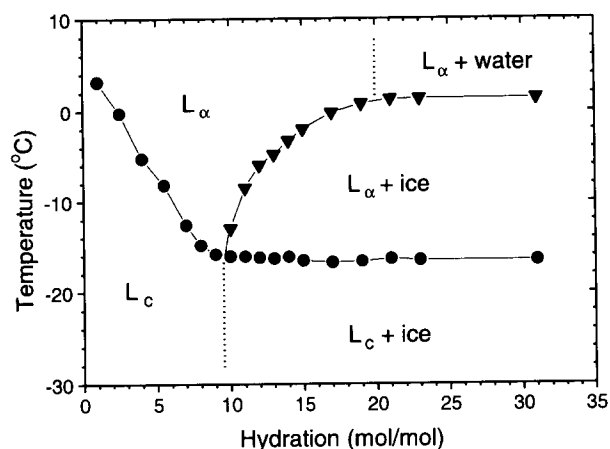


Fig. 2. Phase diagram of the DOPC-water system in the composition range from the monohydrate up to excess hydration ($n_w = 30$ H₂O per lipid) constructed from the peaks in the DSC thermograms in Fig. 1; (●) main lipid phase transition; (▼) ice melting peak. The broken lines indicate the presumed positions of the phase boundaries for saturation of the bilayer surface with water for the gel state (L_c) at $n_w \approx 9$ H₂O and the liquid-crystalline phase (L_α) at $n_w \approx 20$ H₂O.

melting points. At hydration levels above $n_w \approx 20$ H₂O, the ice peak remains fixed at 0°C and gradually increases in height relative to the lipid peak as excess water is added (Fig. 1).

The variations of the lipid and the water phase transition temperatures seen in Fig. 1 are summarized by the phase diagram for DOPC in Fig. 2. The values for the melting point of ice are taken from the shoulder (with an uncertainty of $\pm 1^\circ\text{C}$) or the local maximum, respectively, of the broad transitions seen in Fig. 1. The dotted lines indicate the positions at which the lipid ($n_w \approx 9$ H₂O) and the water transition ($n_w \approx 20$ H₂O) have reached their limiting value, respectively. Although the present study does not reveal the structural nature of the lipid phases, it has been suggested that DOPC and other unsaturated lipids undergo their 'normal' chain-melting transition directly from L_c to L_α [13]. Unlike their saturated analogues they do not appear to pass through a P_β or L_β phase [4]. The lipid phases L_c (condensed or sub-gel lamellar) and L_α (liquid-crystalline lamellar) have thus been assigned in Fig. 2, however for conventional simplicity we will refer to the highly ordered L_c phase as the 'gel state' throughout the text. The assignments of 'water' and 'ice' in Fig. 2 are based on the following arguments concerning the successive melting of first the lipid acyl chains and then the ice, in the course of a DSC heating scan starting with a frozen lipid-water dispersion. It is known that those water molecules which are tightly associated with the surface of the gel state bilayer are 'non-freezable' and do not give rise to a discrete transition in the thermograms. Only when there is an excess of water present in the frozen dispersion, then these

additional molecules show up as an ice-melting peak. Therefore, in the series of thermograms of DOPC with progressively increasing hydration, the first appearance of the ice peak ($n_w \approx 10$ H₂O in Fig. 1) indicates that the surface of the gel phase bilayer has become saturated with water. It is also seen that the DOPC chain-melting temperature reaches its limiting values at this limiting level of hydration, which is indicated in Fig. 2 by the dotted line ($n_w \approx 9$ H₂O). This saturation level for DOPC in the gel state is close to the phase boundary for other, saturated phosphatidylcholines [7–10,21]. Note that any potential correlations of the variation in the lipid phase transition temperature with the changes in the bilayer dimensions or with hydration forces [5,6,20] would reflect the bilayer properties in the gel state and not the fluid phase.

A significant melting point depression is observed for the ice in Figs. 1 and 2, as also reported by others for unsaturated lipid bilayers [22–24]. The melting process of excess ice in a dispersion of DOPC occurs in the presence of liquid-crystalline bilayers, which themselves have already undergone their chain-melting transition. By comparison, in saturated phospholipids the bilayers are still in the gel phase when the ice is melting, and a temperature depression is not usually apparent [7–10] (but see [24]). We conclude that the melting process of excess water in the dispersion depends on the thermal behaviour of the lipid bilayer, i.e., whether its main phase transition temperature lies above or below 0°C.

Generally, it is known that a bilayer in the liquid-crystalline phase has a higher affinity for water than in the gel state, which may be attributed to the increase in molecular area upon the melting of the acyl chains, as well as the occurrence of thermally excited molecular protrusions and bilayer undulations in the liquid-crystalline system [7,8,15,19]. Therefore, as soon as the lipid has passed through its chain-melting transition, the chemical potential is lowered for water molecules near the liquid-crystalline bilayer surfaces. For DOPC, this thermodynamic effect will cause an additional portion of water which was originally present as ice, to melt and to associate with the bilayer surface. That particular fraction of the total water, with its corresponding melting point depression, thus gives rise to the broad ice peak in the thermograms for $n_w \geq 10$ H₂O (Fig. 1). This process, although kinetically controlled and limited by diffusion of the water molecules, occurs rapidly on the timescale of the comparatively slow DSC scan, since we find that thermograms are virtually identical for scanning rates of 1, 2 or 4 degrees per min. The ice melting transition reaches a limiting value of around 0°C at a hydration level near 20 H₂O. This represents the approximate saturation limit for water of the bilayer surface in the liquid-crystalline state, as indicated by the dotted line ($n_w \approx 20$ H₂O) in

the phase diagram in Fig. 2. The hydration limit evaluated from the present DSC approach is not isothermal and corresponds to an unusually low temperature region. Nevertheless, for phosphatidylcholines at ambient temperatures, ^2H -NMR studies of both the lipid head-group and the interbilayer water have suggested a saturation limit for the liquid-crystalline bilayers of around $n_w \approx 23$ [21,25].

Diffraction studies and direct hydration force measurements have shown that uncharged lipid bilayers swell up to a limiting hydration level, at which the attractive and repulsive forces balance another [1,6,15–20]. For both the gel phase and the liquid-crystalline state, any excess water added to the sample is present as a bulk phase in the lipid dispersion, rather than being accommodated within the interbilayer space between two apposing lamellae [7–10,22]. Recent X-ray diffraction studies on DOPC have shown that upon freezing, water molecules are physically squeezed out of the interbilayer space and this process is reversed upon heating, for which a gradual increase in the lamellar repeat distance and a concomitant decrease in the intensity of the ice Bragg peak are reported [22]. In a recent study by ^2H -NMR, the intensity of the D_2O signal in egg lecithin has been monitored as a function of temperature over the broad melting transition of ice, from which the progressive uptake of water molecules into the interbilayer space could be inferred [23]. These complementary observations correlate very well with the present DSC results on the early water transition which exhibits a continual melting point depression as a function of hydration.

The DOPC phase diagram shown in Fig. 2 represents one of the first systematic DSC studies on the hydration of an unsaturated phospholipid over a comprehensive range of water contents (see also [2]). For the saturated dipalmitoylphosphatidylcholine (DPPC), a similar series of DSC thermograms has been published previously [9]. A comparison between the hydration properties of the two synthetic phosphatidylcholines DOPC and DPPC reveals some fundamental analogies. The differences in chain length and unsaturation lead to respective phase transition temperatures for fully hydrated bilayers of $+42.6^\circ\text{C}$ for DPPC [9] and -16.5°C for DOPC (see above), which are in both cases somewhat elevated at low hydration levels. The most notable feature of the saturated lipid, when compared with DOPC, is the occurrence of a pre-transition several degrees beneath the main transition. While this additional peak is generally observed in thermograms of synthetic, saturated acyl-chain lipids [4,5,8,9], it is not present in DOPC or other unsaturated phosphatidylcholines with a main phase transition below zero (see Fig. 1) [2,13,14]. It has been suggested that the pre-transition may be attributed to the co-operative interaction of the bilayer surface with newly incorpo-

rated water [4,9]. That is because it occurs only in the presence of a certain minimum amount of water (approx. 8 H_2O for DPPC), and its temperature then decreases progressively with increasing hydration up to some limiting level (around 14 H_2O for DPPC). This description of the lipid pre-transition resembles closely the behaviour of the ice melting transition which we have observed here for DOPC (see Fig. 2). Therefore it appears that the physical events at the pre-transition in DPPC or other saturated lipids with a chain-melting transition above 0°C , may be regarded analogous to the processes described in the previous paragraphs for the melting of ice in DOPC. On the basis of these arguments it also appears reasonable why DOPC does not exhibit a pre-transition or any tilted $\text{P}_{\beta'}$ or $\text{L}_{\beta'}$ phase. That is because in the frozen DOPC dispersion no water is immediately available that could be incorporated during any lateral expansion preceding the melting of the acyl chains.

Having monitored the melting point depression of the ice transition in DOPC bilayers as a function of hydration, this thermodynamic data can be analyzed quantitatively to characterize the hydration force between the liquid-crystalline bilayers. Various direct hydration force measurements have shown that the repulsive hydration pressure P decays exponentially with the amount n_w of the interbilayer water (or, equivalently, with the interbilayer distance) [1,6,15–20]:

$$P = P_0 \cdot \exp(-n_w/\nu) \quad (1)$$

where P_0 is the nominal hydration pressure at zero hydration, and ν represents the hydration force decay constant in units of water molecules. It is also known that P is directly related to the thermodynamic activity a_w of the interbilayer water [18,19]:

$$P = -(RT/V_w) \cdot \ln(a_w) \quad (2)$$

where V_w is the molar volume of water ($18 \cdot 10^{-6} \text{ m}^3$). Since the absolute transition temperature $T(n_w)$ for the melting of ice varies with hydration over approx. 13 degrees (Fig. 2), this analysis is not an isothermal one and we use $T = T(n_w)$. In an equilibrium situation, the chemical potential is the same for water molecules in the interbilayer space as for those that are accommodated as bulk ice clusters in the dispersion. Generally, the freezing point depression of an aqueous solution, or in this case of the lipid-water dispersion, is then determined by the water activity a_w which itself varies with the hydration level n_w of the sample:

$$\ln(a_w) = (\Delta H_m/R) \cdot [1/T_0 - 1/T(n_w)] \quad (3)$$

where ΔH_m is the molar enthalpy change of melting ice (6.01 kJ/mol), and the absolute temperatures T_0 and $T(n_w)$ represent the melting points of pure water (273.15 K) and of the lipid dispersion, respectively. Combination of Eqs. (2) and (3) leads to the following

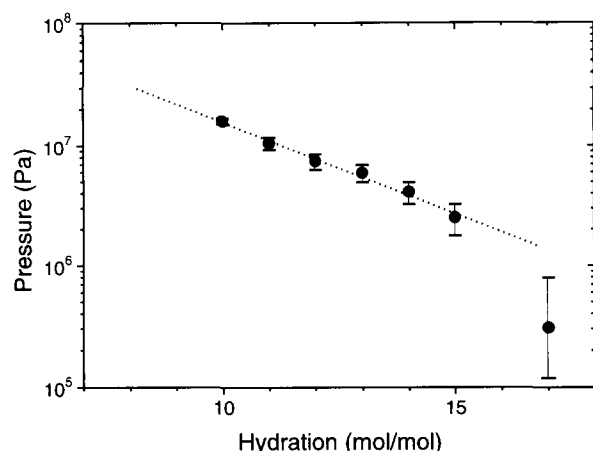


Fig. 3. Logarithmic plot of the hydration pressure versus the amount of water n_w , calculated from the ice melting point depression according to Eq. (4). The inverse slope of the least-squares line-fit (dotted line) gives a (non-isothermal) hydration force decay constant around $\nu \approx 2.8 \text{ H}_2\text{O}$ for liquid-crystalline DOPC bilayers. Error bars indicate the maximum inaccuracy in determining the local maximum of the ice melting transition from the broadened peaks of the thermograms in Fig. 1.

expression, which resembles the force law given by Eq. (1):

$$P = (\Delta H_m/V_w) \cdot [1 - T(n_w)/T_0] \\ = P_0 \cdot \exp(-n_w/\nu) \quad (4)$$

Since the variation of the melting point $T(n_w)$ with hydration n_w is known from the data given in Fig. 2, Eq. (4) can be analyzed by plotting $\log[1 - T(n_w)/T_0]$ as a function of n_w . The expected linear behaviour is demonstrated in Fig. 3, which confirms that the DSC approach describes a genuine hydration force with its typical exponential decay characteristics. The error bars represent the maximum inaccuracy in the determination of the melting point from the local maximum of the broadened ice peak (see Fig. 1). The inverse of the gradient from the least-squares line-fit through the experimental data points in Fig. 3 gives the value of the hydration force decay constant as $\nu \approx 2.8 \pm 0.4 \text{ H}_2\text{O}$ for liquid crystalline DOPC in a temperature range near zero. This result is in fair agreement with the literature values for DOPC at room temperature between 3.3 and 4 H_2O [18,19,26], in view of the fact that the current DSC analysis is based on non-isothermal data. Inspection of Eq. (4) reveals that the nominal hydration pressure P_0 at zero water content must be equal to the quantity $\Delta H_m/V_w$, which makes it $P_0 \approx 3.3 \cdot 10^8 \text{ Pa}$. This theoretically derived result is indeed close to the published experimental values for DOPC at room temperature between $3.0 \cdot 10^8 \text{ Pa}$ and $4.1 \cdot 10^8 \text{ Pa}$ [18,26], and extrapolation of the DSC data in Fig. 3 yields a similar experimental result around $(5.0 \pm 3.0) \cdot$

10^8 Pa . Since the effects of temperature on the hydration force decay length ν and on the value of P_0 are not yet clearly understood, any speculation about the non-isothermal nature of the corresponding values obtained here would be premature. Nevertheless, this DSC approach is based on thermodynamic arguments alone, and there is no need to make any structural or geometrical assumptions about the bilayers as is required for classic hydration force measurements [6,15–20]. It has thus been demonstrated that a thermal analysis of DOPC dispersions as a function of progressive hydration yields quantitative information about the saturation limits and the hydration forces of the lipid bilayers.

4. Acknowledgements

This work has been supported by the grants from the EC, MRC (G9218373MB), SERC (GR/F/69400, GR/F/80852, GR/E/69188, and GR/E/86925) and the Research and Equipment Committee of the University of Oxford.

5. References

- [1] Bryant, G. and Wolfe, J. (1992) *Cryoletters* 14, 23–36.
- [2] Lynch, D.V. and Steponkus, P.L. (1989) *Biochim. Biophys. Acta* 984, 267–272.
- [3] Cevc, G. (1992) in *Hydration of Biological Macromolecules* (Westhof, E., ed.), pp. 338–390, Macmillan Press, New York.
- [4] Cevc, G. (1991) *Biochim. Biophys. Acta* 1062, 59–69.
- [5] Cevc, G. (1988) *Ber. Bunsenges. Phys. Chem.* 92, 953–961.
- [6] Cevc, G. and Marsh, D. (1985) *Biophys. J.* 47, 21–31.
- [7] Chapman, D., Williams, R.M. and Ladbroke, B.D. (1967) 8 *Chem. Phys. Lipids* 1, 445–475.
- [8] Janiak, M.J., Small, D.M. and Shipley, G.G. (1979) *J. Biol. Chem.* 254, 6068–6078.
- [9] Kodama, M., Kuwabara, M. and Seki, S. (1982) *Biochim. Biophys. Acta* 689, 567–570.
- [10] Small, D.M. (1967) *J. Lipid Res.* 8, 551–557.
- [11] Ulmius, J., Wennerström, H., Lindblom, G. and Arvidson, G. (1977) *Biochem. J.* 16, 5742–5745.
- [12] Watts, A. and Spooner, P.J.R. (1991) *Chem. Phys. Lipids* 57, 195–211.
- [13] Keough, K.M.W. and Kariel, N. (1987) *Biochim. Biophys. Acta* 902, 11–18.
- [14] Lewis, R.N.A.H., Sykes, B.D. and McElhaney, R.N. (1988) *Biochemistry* 27, 880–887.
- [15] Israelachvili, J.N. and Wennerström, H. (1992) *J. Phys. Chem.* 96, 520–531.
- [16] Leikin, S., Parsegian, V.A., Rau, D.C. and Rand, R.P. (1993) *Annu. Rev. Phys. Chem.* 44, 369–395.
- [17] LeNeveu, D.M., Rand, R.P. and Parsegian, V.A. (1976) *Nature* 259, 601–603.
- [18] Marsh, D. (1989) *Biophys. J.* 55, 1093–1100.
- [19] Rand, R.P. and Parsegian, V.A. (1989) *Biochim. Biophys. Acta* 988, 351–376.
- [20] Simon, S.A., Fink, C.A., Kenworthy, A.K. and McIntosh, T.J. (1991) *Biophys. J.* 59, 538–546.

- [21] Ulrich, A.S. and Watts, A. (1994) *Biophys. J.* in press.
- [22] Gleeson, J.T., Wall, M.E., Erramilli, S. and Gruner, S.M. (1993) *Biophys. J.* 64, A295.
- [23] Yan, Z., Pope, J. and Wolfe, J. (1993) *Faraday Trans.* 89, 2583–2588.
- [24] Ter-Minassian-Saraga, L. and Madelmont, G. (1982) *J. Coll. Interf. Sci.* 85, 375–388.
- [25] Gawrisch, K., Richter, W., Möps, A., Balgavy, P., Arnold, K. and Klose, G. (1985) *Stud. Biophys.* 108, 5–16.
- [26] Ulrich, A.S. and Watts, A. (1994) *Biophys. Chem.* 49, 39–50.